

On filtration a red colored solution was obtained and from the absorbance value (using $\epsilon_{496} = 21\,300$) the concentration of TPM^-K^+ , and hence of KH, was obtained. The resulting values of the solubility of KH showed appreciable variation in six determinations, as may be expected for a very sparingly soluble substance. The overall result for the solubility of potassium hydride in the THF/crown ether system is $(21.5 \pm 9.5) \times 10^{-6}$ M.

The solubility of H_2 in THF was determined by the GLC method described by Symons³⁴ under conditions analogous to those pertaining to the reaction under study. Thus, H_2 gas was introduced to 1 atm into the reaction vessel containing ~20 mL of THF after freezing with liquid nitrogen and evacuating the system. The vessel was then closed off from the H_2 source, allowed to reach room temperature, and shaken thoroughly. Aliquots (4 mL) of the solution were then removed with a gas-tight syringe and the gas stripped off by the technique described previously.³⁴ Analysis was performed by GLC using a prior calibration with a known volume of H_2 . The solubility of H_2 in THF at 25 °C was thus obtained as $(3.66 \pm 0.20) \times 10^{-3}$ M. The solubility coefficient can then be expressed as the volume of gas dissolved by unit volume of liquid, i.e., $22.4 \times 3.66 \times 10^{-3} = 0.082$.

Acknowledgment. Financial support of this research by the National Research Council of Canada and Atomic Energy of Canada Limited is gratefully acknowledged, as are discussions with Drs. J. H. Rolston, D. R. Smith, and E. A. Symons (AECL), and Professors F. G. Bordwell, E. Grovenstein, and A. Streitwieser.

References and Notes

- (1) Part 5: E. Buncel and B. C. Menon, *Can. J. Chem.*, **54**, 3949 (1976).
- (2) H. O. House, "Modern Synthetic Reactions", 2nd ed, W. A. Benjamin, Menlo Park, Calif., 1972.
- (3) E. M. Kaiser and D. W. Sloacum, in "Organic Reactive Intermediates", S. P. McManus, Ed., Academic Press, New York, N.Y., 1973.
- (4) D. J. Cram, "Fundamentals of Carbanion Chemistry", Academic Press, New York, N.Y., 1965.
- (5) R. P. Bell, "The Proton in Chemistry", 2nd ed, Cornell University Press, Ithaca, N.Y., 1973.
- (6) J. R. Jones, "The Ionization of Carbon Acids", Academic Press, London, 1973.
- (7) E. Buncel, "Carbanions. Mechanistic and Isotopic Aspects", Elsevier, Amsterdam, 1975.
- (8) E. Buncel and E. A. Symons, *J. Org. Chem.*, **38**, 1201 (1973); *Chem. Commun.*, 771 (1967); *Can. J. Chem.*, **44**, 771 (1966).
- (9) E. Buncel, K. E. Russell, and J. Wood, *Chem. Commun.*, 252 (1968); E. Buncel and A. W. Zabel, *J. Am. Chem. Soc.*, **89**, 3082 (1967); E. Buncel, E. A. Symons, and A. W. Zabel, *Chem. Commun.*, 173 (1965).
- (10) E. A. Symons and E. Buncel, *J. Am. Chem. Soc.*, **94**, 3641 (1972); *Can. J. Chem.*, **51**, 1673 (1973); E. Buncel and E. A. Symons, *J. Am. Chem. Soc.*, **98**, 656 (1976).
- (11) J. M. Flournoy and W. K. Wilmarth, *J. Am. Chem. Soc.*, **83**, 2257 (1961).
- (12) U. Schindewolf, *J. Chim. Phys. Phys.-Chim. Biol.*, **60**, 124 (1963).
- (13) K. O'Donnell, R. Bacon, K. L. Chellappa, R. L. Schowen, and J. K. Lee, *J. Am. Chem. Soc.*, **94**, 2500 (1972).
- (14) R. G. Pearson and J. Songstad, *J. Am. Chem. Soc.*, **89**, 1827 (1967).
- (15) E. Buncel and B. C. Menon, *Chem. Commun.*, 648 (1976).
- (16) C. A. Brown, *J. Org. Chem.*, **39**, 3913 (1974).
- (17) E. Wiberg and A. Amberger, "Hydrides of the Elements of Main Groups I-IV", Elsevier, Amsterdam, 1971.
- (18) C. J. Pedersen and H. K. Frensdorff, *Angew. Chem., Int. Ed. Engl.*, **11**, 16 (1972).
- (19) D. J. Sam and H. E. Simmons, *J. Am. Chem. Soc.*, **96**, 2252 (1974).
- (20) C. L. Liotta and H. P. Harris, *J. Am. Chem. Soc.*, **96**, 2250 (1974).
- (21) C. L. Liotta, E. E. Grisdale, and H. P. Hopkins, Jr., *Tetrahedron Lett.*, 4205 (1975).
- (22) G. Gau and S. Marques, *J. Am. Chem. Soc.*, **98**, 1538 (1976).
- (23) A. Streitwieser, Jr., J. R. Murdoch, G. Häfelinger, and C. J. Chang, *J. Am. Chem. Soc.*, **95**, 4248 (1973).
- (24) E. Buncel and B. C. Menon, unpublished work.
- (25) M. Szwarc, A. Streitwieser, Jr., and P. C. Mowery, *Ions Ion Pairs Org. React.*, **2** (1974).
- (26) J. Smid, *Ions Ion Pairs Org. React.*, **1** (1972).
- (27) An indirect estimate of K_6/K_7 can be made in the following way. The complexation constants K_i of fluorenyl alkali metal salts in THF/dicyclohexyl-18-crown-6 ether have been found²⁶ to vary between 10^4 and 10^6 M^{-1} , so that one might also expect for DXM^-K^+ in the THF/18-crown-6 system $K_i \approx 10^4$ – 10^6 M^{-1} . Complexation constants of potassium salts in THF have not been reported, but K_i is known¹⁸ for KCl in MeOH/18-crown-6 as 10^6 M^{-1} , and extrapolating to the lower dielectric constant THF would increase K_i to $\sim 10^7$ M^{-1} . The K_i value for KH would be expected to be somewhat smaller (comparable to that of KBr), $\sim 10^6$ M^{-1} . On this basis we estimate that the K_6/K_7 ratio pertaining to DXM^-K^+ and H^-K^+ in the THF/18-crown-6 system would range between 1 and 10^{-2} .
- (28) W. S. Matthews, J. E. Bares, J. E. Bartmess, F. G. Bordwell, F. J. Cornforth, G. E. Drucker, Z. Margolin, R. J. McCallum, G. J. McCollum, and N. R. Vanier, *J. Am. Chem. Soc.*, **97**, 7006 (1975).
- (29) K. Bowden and R. Stewart, *Tetrahedron*, **21**, 261 (1965); R. A. Cox and R. Stewart, *J. Am. Chem. Soc.*, **98**, 488 (1976).
- (30) C. D. Ritchie, in "Solute-Solvent Interactions", J. F. Coetzee and C. D. Ritchie, Ed., Marcel Dekker, New York, N.Y., 1969.
- (31) E. Buncel and H. Wilson, *Adv. Phys. Org. Chem.*, in press.
- (32) M. Eigen, *Angew. Chem., Int. Ed. Engl.*, **3**, 1 (1964).
- (33) L. Gordon, P. May, and R. Lee, *Ind. Eng. Chem.*, **51**, 1257 (1959).
- (34) E. A. Symons, *Can. J. Chem.*, **49**, 3940 (1971).

Hydrazine Lone Pair-Lone Pair Interactions. X-Ray Crystallographic Structure Determination of Two Six-Membered Ring Hydrazines

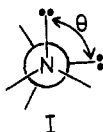
S. F. Nelsen,* W. C. Hollinsed, and J. C. Calabrese

Contribution from the Department of Chemistry, University of Wisconsin, Madison, Wisconsin 53706. Received January 19, 1977

Abstract: The structures, determined by x-ray crystallography, are reported for 3,4-dimethyl-3,4-diazabicyclo[4.4.0]decane (**2**) and for 2,3-dimethyl-2,3-diazatricyclo[8.4.0.0^{4,9}]tetradec-9-ene (**3**). Crystals of **2** are triclinic, $P\bar{1}$, with $a = 9.618$ (2), $b = 10.435$ (2), $c = 5.440$ (1) Å, $\alpha = 102.55$ (2), $\beta = 94.38$ (1), $\gamma = 74.88$ (2)°, $V = 514.4$ (2) Å³, and $Z = 2$. The structure was solved by direct methods and refined to $R_1 = 4.6\%$ and $R_2 = 5.7\%$ for 666 independent observed reflections. Crystals of **3** are monoclinic, $P2_1/n$, with $a = 14.343$ (3), $b = 6.672$ (1), $c = 14.073$ (2) Å, $\beta = 104.29$ (1)°, $V = 1304.9$ (3) Å³, and $Z = 4$. Solution by direct methods and refinement gave $R_1 = 5.4\%$ and $R_2 = 5.7\%$ for 1398 independent observed reflections. Compound **2** has the methyl groups substituted diequatorial on the six-membered ring and **3** has the axial, equatorial conformation. The implications of these results for the interpretation of photoelectron spectroscopic experiments and equilibrium constant measurements are discussed.

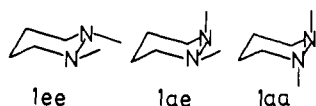
The conformations of hydrazine derivatives have received a great deal of study by a wide range of experimental techniques.¹ The angle of rotation about the N-N bond has been of particular interest, and it is well established that for many

acyclic hydrazine derivatives, the preferred conformation is that which has the lone-pair orbitals nearly perpendicular (I, θ near 90°), although this is clearly not the sterically least hindered conformation. A large change in the energy separa-



tion of the two highest occupied molecular orbitals (which are dominated by the lone pair atomic orbitals) occurs as θ is changed, and photoelectron spectroscopy (PES) studies^{2,3} have shown that this separation is about 2.3 eV when θ is near 0 to 180°, but drops to about 0.5 eV when θ is near 90°. This sensitivity of the lone pair–lone pair energy separation to θ has led to the use of PES to determine hydrazine conformation, by using a scaled estimated curve derived from MO calculations. The calculated energy separation for a given value of θ is, however, dependent upon the geometry at nitrogen,^{3d} since the separation depends on the overlap of the lone pair atomic orbitals. Experimental evidence on the extent of any dependence of the degree of flattening at nitrogen on θ has previously been lacking.

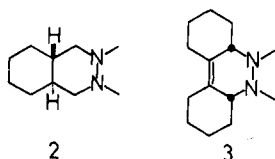
Six-membered ring hydrazines offer an especially good opportunity for study of the influence of steric and electronic effects upon hydrazine geometry. The cyclic structure requires that the ring substituents exist in well defined axial and equatorial positions. The PE spectrum of 1,2-dimethylhexahydropyridazine showed the presence of a predominate component with a 2.3-eV lone pair–lone pair energy separation, hence assigned to the trans lone pair diequatorial methyl conformation **1ee**, and a minor component having about a 1-eV separation, expected for either of the gauche lone pair conformations **1ae** or **1aa**.^{2,3} Subsequent ¹³C NMR studies showed



unambiguously that **1ee** predominates slightly in solution, and that **1aa** is not present in detectable concentration at low temperature,⁴ as expected on steric grounds. There is a fine balance between steric and electronic effects in **1**, and introduction of methyl groups at the carbons α to the nitrogens causes a strong preference for ae conformations, as has been shown both by PES^{3b,3e} and ¹³C NMR^{4b,5} spectroscopy, which have been in agreement as to the predominant conformation present in all cases examined.

Construction of a hexahydropyridazine ring using all tetrahedral angles and standard bond lengths^{4c} suggested that the dihedral angle between ee nitrogen substituents would be smaller than that between ae substituents, but real hexahydropyridazine geometry remained unknown.

We therefore decided to determine structure by x-ray crystallography to answer the geometrical questions raised above. Of the very few solid tetraalkylhydrazines known, we selected **2** and **3** for study. Although **2** has a quite small dif-



ference in ΔH° between the ee and ae forms in solution,^{4b} models suggested that the ee form would pack better, and that the solid might consist of this conformation. Proton NMR work on **3** was unable to show which conformation this compound prefers in solution,⁶ but *cis*- α,α' -dimethyl substitution provides a strong ae preference in hexahydropyridazines,^{4b,5} as does the presence of β,β' -unsaturation,¹ so it seemed likely that **3** would strongly prefer the ae dimethyl conformation in solution, and perhaps also in the solid.

Experimental Section

Single Crystal X-Ray Structure of 3,4-Dimethyl-3,4-diazabicyclo[4.4.0]decane (2). A crystal of 3,4-dimethyl-3,4-diazabicyclo[4.4.0]decane (**2**) grown by sublimation (parallelepiped with dimensions 0.38 × 0.30 × 0.20 mm) was mounted in a glass capillary under argon and placed on a Syntex P1 four-circle computer-controlled diffractometer. Lattice constants were obtained from 15 diffraction maxima well distributed in 2θ , χ , and ω . Graphite monochromated Mo K α (0.7107 Å) radiation was used through the alignment and data collection procedures. The Syntex routines⁷ indicated a triclinic unit cell with $a = 9.618$ (2), $b = 10.435$ (2), $c = 5.440$ (1) Å, $\alpha = 102.55$ (2), $\beta = 94.38$ (1), $\gamma = 74.88$ (2)°, and $V = 514.4$ (2) Å³. The lattice constants and Laue symmetry were verified by partial rotation photographs along each of the reciprocal axes. The density of the compound was not measured due to the unusual solubility of the compound in most aqueous and organic solvents. The calculated density of **2** is 1.086 g/cm³ with $Z = 2$ (centrosymmetric P1 space group).

Intensity data were collected in the range $2^\circ \leq 2\theta \leq 45^\circ$ using a scan speed mode (2–24°/min) which varied according to the intensity of the measurement. The intensities of two standard reflections were monitored every 50 reflections and showed no significant decay in intensity throughout the collection of data.

The data were reduced as previously described⁸ to yield 1136 independent reflections, of which 666 were considered significantly above background (with $I > 2\sigma(I)$) and used in the solution and refinement of the structure.

The solution of the structure was accomplished by direct methods.⁹ Isotropic full-matrix least-squares refinement of the nonhydrogen atoms converged at $R_1 = 16.4\%$ and $R_2 = 20.3\%$.^{9–11} These coordinates were used in a difference map which revealed the positions of the 20 hydrogen atoms. Isotropic full-matrix least-squares refinement for all atoms converged at $R_1 = 7.6\%$ and $R_2 = 9.2\%$. The final full-matrix least-squares refinement which included nonhydrogen atoms with anisotropic thermal motion and hydrogens with isotropic thermal parameters resulted in $R_1 = 4.6\%$ and $R_2 = 5.7\%$. All hydrogen distances were normal and ranged from 0.89 to 1.08 Å. A final difference map resulted in no peak greater than 0.1 e, and the standard deviation in an observation of unit weight ("goodness of fit" value) was 1.48.

Single Crystal X-Ray Structure of 2,3-Dimethyl-2,3-diazabicyclo[8.4.0.0^{4,9}]tetradec-9-ene (3). Crystals of 2,3-dimethyl-2,3-diazabicyclo[8.4.0.0^{4,9}]tetradec-9-ene (**3**) were grown by sublimation over a period of 4–5 days. An octahedral shaped crystal (0.40 × 0.25 × 0.25 mm) was mounted in a glass capillary under argon and placed on a Syntex P1 four-circle computer-controlled diffractometer. The crystal was optically centered and 15 diffraction maxima were automatically centered in 2θ , χ , and ω . Graphite monochromated Mo K α ($\lambda = 0.7107$ Å) radiation was used throughout the alignment and data collection procedures. The Syntex routines⁷ indicated a monoclinic unit cell with $a = 14.343$ (3), $b = 6.672$ (1), $c = 14.073$ (2) Å, $\beta = 104.29$ (1)°, and $V = 1304.9$ (3) Å³. Systematic absences ($0k0$) with k odd and ($h0l$) with $h + l$ odd indicated the space group $P2_1/n$ (nonstandard setting of $P2_1/c$ (C_{2h}^5 , No. 14). Equivalent positions: $\pm[x, y, z; 1/2 - x, 1/2 + y, 1/2 - z]$. The monoclinic symmetry and associated lattice constants were verified by partial rotation photographs along each of the three reciprocal axes. The density of the compound was not measured due to the unusual solubility of the compound in most organic and aqueous solvents. The calculated density for **3** having $Z = 4$ is 1.122 g/cm³.

Intensity data were collected in the range $2^\circ \leq 2\theta \leq 50^\circ$ using a variable scan speed mode of 2–24°/min. The intensities of two standard reflections were monitored every 50 reflections and showed no significant decay throughout data collections. The data were reduced as previously described⁸ to yield 2495 independent reflections, of which 1398 were considered significantly above background (with $I > 2\sigma(I)$) and used in the solution and refinement of the structure.

The solution of the structure was accomplished by direct methods.⁹ Isotropic full-matrix least-squares refinement of the nonhydrogen atoms converged at $R_1 = 14.1\%$ and $R_2 = 18.2\%$.^{9–11} These coordinates were used in a difference map which revealed the hydrogen atoms. Isotropic full-matrix least-squares refinement of all the atoms converged at $R_1 = 8.0\%$ and $R_2 = 8.9\%$. Further refinement with anisotropic temperature factors for the nonhydrogen atoms resulted in $R_1 = 5.4\%$ and $R_2 = 5.7\%$. C–H distances ranged from 0.94 to 1.02 Å. A final difference map resulted in no peak greater than 0.2 e, and the final "goodness of fit" value was 1.28.

Table I. Fractional Coordinates ($\times 10^4$) and Isotropic Temperature Factors¹¹ for **2**^a

Atom	x	y	z	B_{iso}
C(1)	5610 (4)	2137 (4)	3611 (9)	
C(2)	4218 (4)	1774 (4)	2702 (10)	
N(3)	2952 (3)	2890 (3)	3531 (7)	
N(4)	2952 (3)	3117 (3)	6324 (7)	
C(5)	4232 (4)	3603 (5)	7298 (10)	
C(6)	5604 (4)	2564 (4)	6457 (8)	
C(7)	6969 (5)	3005 (5)	7436 (10)	
C(8)	8318 (5)	1899 (6)	6527 (10)	
C(9)	8306 (5)	1451 (6)	3688 (10)	
C(10)	6935 (5)	1027 (5)	2699 (10)	
C(11)	1667 (5)	2422 (6)	2543 (13)	
C(12)	1688 (5)	4209 (6)	7225 (14)	
H(1a)	5622 (28)	2978 (31)	3019 (56)	2.9 (7)
H(2a)	4118 (34)	940 (36)	3218 (72)	5.2 (10)
H(2e)	4125 (28)	1678 (28)	861 (58)	2.6 (8)
H(5a)	4169 (33)	4431 (37)	6531 (71)	5.2 (10)
H(5e)	4227 (40)	3837 (43)	9040 (78)	6.7 (13)
H(6a)	5579 (27)	1720 (30)	6946 (57)	2.8 (7)
H(7a)	6938 (32)	3832 (32)	6707 (62)	4.1 (9)
H(7e)	6911 (35)	3214 (39)	9103 (71)	4.5 (11)
H(8a)	8448 (35)	1088 (37)	7231 (67)	4.7 (10)
H(8e)	9118 (42)	2262 (36)	7290 (73)	5.9 (11)
H(9a)	8388 (32)	2220 (36)	2967 (66)	4.3 (9)
H(9e)	9076 (45)	721 (46)	3124 (88)	7.7 (14)
H(10a)	6862 (34)	207 (35)	3168 (68)	4.3 (10)
H(10e)	6995 (33)	814 (35)	963 (65)	4.0 (10)
H(11a)	1556 (38)	1664 (38)	3362 (75)	6.0 (13)
H(11b)	1842 (45)	2068 (47)	802 (81)	7.1 (15)
H(11c)	818 (47)	3318 (48)	3175 (91)	8.5 (13)
H(12a)	1763 (45)	4491 (47)	8888 (87)	6.8 (15)
H(12b)	1640 (38)	5069 (41)	6549 (80)	6.2 (12)
H(12c)	840 (41)	3769 (37)	6833 (74)	5.8 (11)

^a Standard deviations of the last significant figure are given in parentheses in this and in all following tables and figures.

Table II. Anisotropic Temperature Factors¹¹ for **2** ($\times 10^4$)^a

Atom	β_{11}	β_{22}	β_{33}	β_{12}	β_{13}	β_{23}
C(1)	110 (6)	77 (6)	399 (26)	-22 (4)	33 (9)	36 (10)
C(2)	127 (6)	102 (6)	361 (25)	-39 (5)	-19 (9)	49 (11)
N(3)	103 (5)	107 (5)	436 (21)	-26 (3)	-19 (7)	57 (8)
N(4)	103 (5)	115 (5)	458 (22)	-16 (4)	29 (7)	65 (8)
C(5)	125 (7)	96 (6)	437 (29)	-24 (5)	13 (10)	51 (12)
C(6)	115 (6)	83 (6)	349 (26)	-27 (5)	-6 (8)	47 (9)
C(7)	135 (7)	122 (7)	398 (29)	-40 (5)	-31 (10)	49 (12)
C(8)	112 (6)	175 (8)	590 (31)	-44 (6)	-54 (11)	142 (13)
C(9)	113 (7)	151 (8)	558 (30)	-16 (6)	19 (11)	113 (13)
C(10)	125 (6)	118 (7)	369 (26)	-31 (5)	42 (9)	21 (11)
C(11)	119 (7)	155 (9)	652 (37)	-42 (6)	-4 (12)	19 (15)
C(12)	133 (8)	137 (8)	658 (37)	-13 (6)	54 (13)	23 (15)

^a Anisotropic temperature factors are of the form: $\exp[-(\beta_{11}h^2 + \beta_{22}k^2 + \beta_{33}l^2 + 2\beta_{12}hk + 2\beta_{13}hl + 2\beta_{23}kl)]$.

Results and Discussion

Coordinates and thermal parameters for compound **2** are given in Tables I and II, those for compound **3** are given in Tables III and IV. Bond lengths, bond angles, and torsional angles for **2** and **3** are given in Figures 1–3 and 4–6, respectively. Observed and calculated structure factors for each compound are also given (see paragraph at end of paper regarding supplementary material).

A thermal ellipsoid plot of compound **2** (Figure 7) shows the ee form to be favored in the crystalline state over the ae form as expected from steric considerations. A similar plot of compound **3** (Figure 8) shows it to prefer the ae conformation in the solid state.

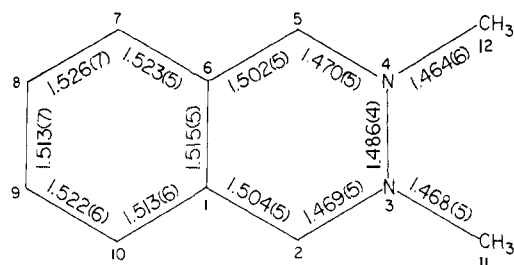
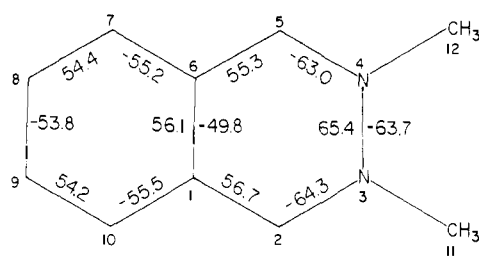
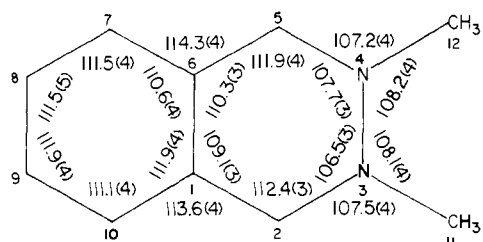
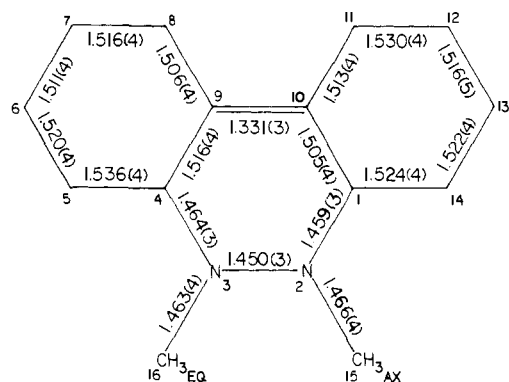
The comparison of geometry at the hydrazine units in the trans and gauche lone pair hydrazines **2** and **3**, respectively,

is a principal point of interest in this work, and will be the focus of our discussion. Because θ is constrained to be about 180° for the ee hydrazine **2**, it will have a larger lone pair–lone pair interaction than the ae compound **3** (PE studies of close models show that the energy separations should be about 2.3 and 1.0 eV, respectively). Since equilibration studies indicate that the ee conformation is electronically destabilized relative to ae conformations, one might imagine that the geometry at the nitrogens of **2** would be distorted relative to that of **3** in order to minimize lone pair–lone pair interaction. The geometry changes which would minimize interaction of the lone pairs are lengthening of the N–N bond and increasing the nonplanarity at nitrogen, both of which decrease the lone pair–lone pair overlap. Our data allow evaluation of the size of these effects.

Allman¹² has discussed the differences in bond length ex-

Table III. Fractional Coordinates ($\times 10^4$) and Isotropic Temperature Factors¹¹ for **3**

Atom	x	y	z	B_{iso}
C(1)	2032 (2)	-592 (4)	3690 (2)	
N(2)	2787 (2)	780 (3)	3567 (2)	
N(3)	3027 (2)	2049 (3)	4429 (2)	
C(4)	3491 (2)	965 (4)	5326 (2)	
C(5)	3517 (3)	2346 (5)	6206 (2)	
C(6)	3841 (3)	1316 (5)	7196 (2)	
C(7)	3238 (2)	-520 (5)	7245 (2)	
C(8)	3261 (2)	-1935 (5)	6408 (2)	
C(9)	2944 (2)	-940 (4)	5419 (2)	
C(10)	2246 (2)	-1605 (4)	4677 (2)	
C(11)	1543 (2)	-3278 (5)	4710 (3)	
C(12)	527 (2)	-2400 (6)	4482 (3)	
C(13)	288 (2)	-1230 (5)	3529 (3)	
C(14)	1036 (2)	359 (5)	3481 (3)	
C(15)	3611 (2)	-307 (6)	3377 (3)	
C(16)	3570 (3)	3787 (5)	4229 (3)	
H(1a)	2037 (17)	-1695 (40)	3201 (19)	3.2 (6)
H(4a)	4181 (16)	649 (32)	5346 (15)	2.0 (5)
H(5a)	2863 (21)	2950 (41)	6115 (20)	4.4 (7)
H(5e)	3939 (21)	3484 (47)	6201 (21)	5.1 (8)
H(6a)	4532 (20)	895 (40)	7332 (19)	4.3 (6)
H(6e)	3787 (20)	2258 (45)	7695 (23)	4.6 (7)
H(7a)	2564 (19)	-134 (37)	7179 (17)	3.1 (6)
H(7e)	3432 (20)	-1133(45)	7902 (23)	4.7 (7)
H(8a)	3957 (20)	-2366 (39)	6478 (19)	3.8 (6)
H(8e)	2904 (20)	-3157 (45)	6450 (20)	4.3 (7)
H(11a)	1619 (20)	-4305 (48)	4225 (22)	5.1 (7)
H(11e)	1693 (18)	-3926 (40)	5349 (20)	4.0 (7)
H(12a)	477 (17)	-1520 (42)	5034 (19)	4.1 (6)
H(12e)	48 (23)	-3524 (52)	4435 (23)	6.1 (9)
H(13a)	-344 (21)	-562 (44)	3443 (21)	4.8 (7)
H(13e)	245 (19)	-2195 (42)	2974 (21)	4.6 (7)
H(14a)	997 (18)	1439 (41)	3936 (20)	4.1 (6)
H(14e)	930 (18)	924 (40)	2855 (22)	3.3 (6)
H(15a)	4130 (25)	687 (51)	3342 (24)	6.5 (9)
H(15b)	3409 (21)	-973 (49)	2772 (25)	5.0 (8)
H(15c)	3922 (18)	-1311 (43)	3888 (21)	4.1 (7)
H(16a)	3587 (21)	4859 (50)	4739 (25)	6.3 (9)
H(16b)	4263 (25)	3421 (48)	4228 (23)	6.2 (8)
H(16c)	3273 (21)	4227 (47)	3587 (25)	5.3 (8)

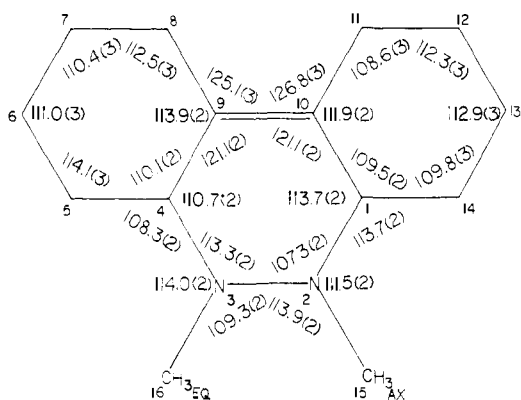
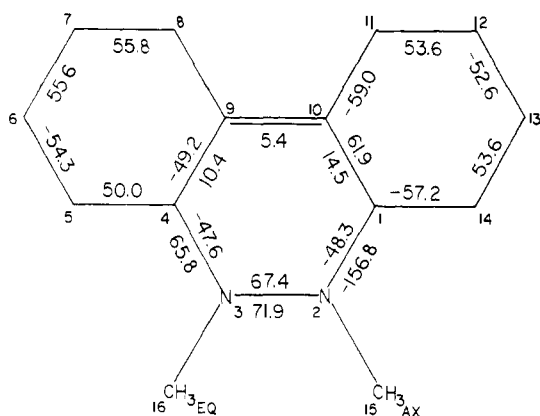
**Figure 1.** Bond lengths for compound **2**.¹¹**Figure 3.** Torsional angles for compound **2**.¹¹**Figure 2.** Bond angles for compound **2**.¹¹**Figure 4.** Bond lengths for compound **3**.¹¹

pected from the use of different experimental techniques for measurement. For hydrazine itself, which has a lone pair-lone pair dihedral angle θ near 95° , very similar N-N bond lengths

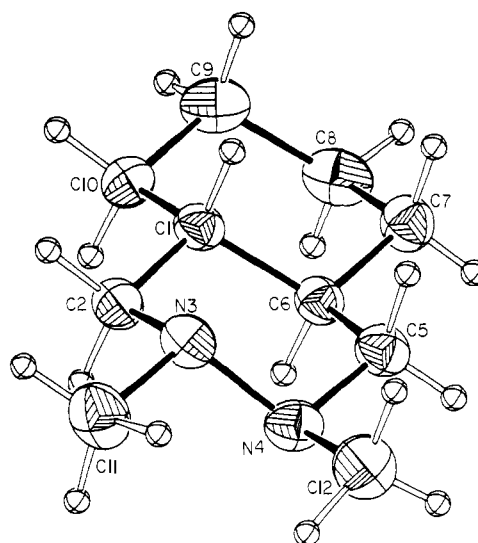
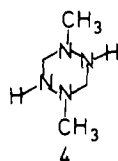
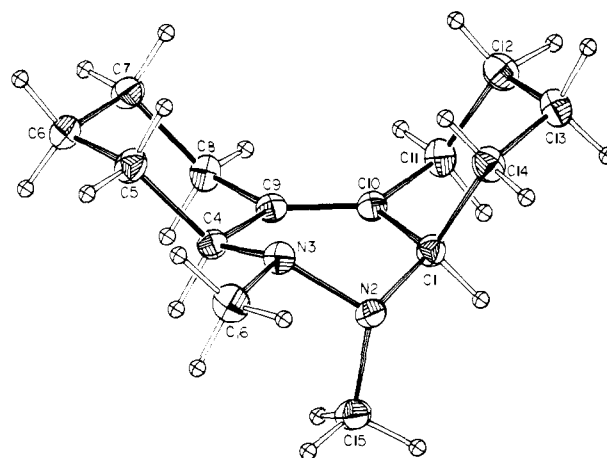
Table IV. Anisotropic Temperature Factors¹¹ for 3^a

Atom	β_{11}	β_{22}	β_{33}	β_{12}	β_{13}	β_{23}
C(1)	42 (2)	170 (7)	43 (2)	-3 (3)	8 (1)	-10 (3)
N(2)	44 (1)	188 (6)	41 (1)	3 (2)	14 (1)	-7 (3)
N(3)	47 (1)	135 (6)	49 (2)	-2 (2)	13 (1)	0 (2)
C(4)	38 (2)	155 (7)	47 (2)	9 (3)	10 (1)	-12 (3)
C(5)	61 (2)	179 (8)	52 (2)	-10 (4)	15 (2)	-24 (3)
C(6)	57 (2)	267 (10)	48 (2)	-4 (4)	12 (2)	-36 (4)
C(7)	53 (2)	264 (9)	42 (2)	10 (4)	13 (2)	-4 (4)
C(8)	53 (2)	179 (8)	47 (2)	1 (3)	6 (1)	2 (3)
C(9)	39 (1)	131 (7)	43 (2)	16 (3)	12 (1)	1 (3)
C(10)	39 (2)	128 (6)	45 (2)	12 (3)	10 (1)	-6 (3)
C(11)	52 (2)	167 (8)	54 (2)	-8 (3)	5 (2)	5 (4)
C(12)	46 (2)	241 (9)	75 (3)	-16 (4)	15 (2)	12 (4)
C(13)	40 (2)	237 (9)	67 (2)	0 (3)	2 (2)	1 (4)
C(14)	44 (2)	230 (9)	51 (2)	13 (3)	5 (2)	25 (4)
C(15)	54 (2)	259 (9)	56 (2)	12 (4)	22 (2)	-9 (4)
C(16)	66 (2)	198 (9)	65 (3)	-16 (4)	20 (2)	16 (4)

^a Anisotropic temperature factors are of the form: $\exp[-(\beta_{11}h^2 + \beta_{22}k^2 + \beta_{33}l^2 + 2\beta_{12}hk + 2\beta_{13}hl + 2\beta_{23}kl)]$.

Figure 5. Bond angles for compound 3.¹¹Figure 6. Torsional angles for compound 3.¹¹

have been calculated using x-ray¹³ ($r_x = 1.46 \text{ \AA}$), far infrared¹⁴ ($r_0 = 1.453 (5)$), and electron diffraction¹⁵ ($r_g = 1.449 (4)$) data. The only other accurate N-N bond length for a hydrazine with saturated alkyl and hydrogen substitution is the x-ray value of $1.447 (3)$ ¹⁶ for the gauche lone pair hydrazine 4

Figure 7. Thermal ellipsoid plot of compound 2 showing numbering and 30% probability ellipsoids.⁹Figure 8. Thermal ellipsoid plot of compound 3 showing numbering and 20% probability ellipsoids.⁹

(which crystallizes with axial NH bonds and equatorial methyls), in excellent agreement. Similarly, the N-N bond length determined here for the gauche-tetraalkylhydrazine, $1.450 (3)$, is in complete agreement with the other gauche

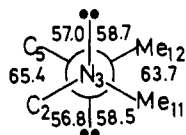
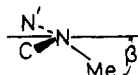


Figure 9. Newman projection along the N(3)–N(4) bond in compound 2.

hydrazine values. The observed N–N bond length for the *trans*-hydrazine **2** was 1.486 (4) Å. Allman¹² has discussed evidence that x-ray bond distances are increased for bonds to nitrogen atoms because of displacement of the observed center of electron density toward the lone pair. This would tend to increase the x-ray bond length for a *trans* relative to a *gauche* hydrazine, but any such effect seems to be quite small, from the data quoted above for hydrazine. Although the N–N bond length may be slightly greater for *trans* than for the *gauche* hydrazines, such an effect is seen to be rather small from our observed difference in N–N bond length for **2** and **3** being about 0.04 Å, representing nine standard deviations.

The bond angles about the nitrogen atoms change far more significantly between **2** and **3**, as expected because angular deformation is easier than bond length deformation. The degree of flattening at nitrogen may be examined conveniently by comparing the values of β , the angle of bend of the *N*-methyl group out of the CNN' plane ($\beta = 54.7^\circ$ for a tetra-



hedral atom, 0° for a planar one). For the *trans*-hydrazine **2**, the β values at the two nitrogens are 59.3 and 59.0° , or about 4.4° larger than the tetrahedral value, while for **3**, β values of 49.4° (N(2)Me(15) (axial)) and 47.8° (N(3)Me(16) (equatorial)) are observed, 5.3 and 6.9° lower than a tetrahedral nitrogen would show. One factor favoring increased bending in **2** compared to **3** is that this bending increases the MeNNMe dihedral angle, relieving the Me,Me steric interaction for **2**. The steric situation is more complicated for **3**, where both the interaction with the ring C(4) carbon and Me(16) will be affected as Me(15) (eq) is moved. While the internal C(1)N(2)N(3) angle (at the nitrogen with the axial methyl) is 5° less than the C(4)N(3)N(2) (equatorial methyl) angle, changes in the external bond angles result in similar degrees of flattening at the nitrogens (β values within 1.6°). This suggests that the change in β between **2** and **3** is not entirely steric, but partly a result of the change in lone pair–lone pair interaction because θ is different. The β angle at the N–Me nitrogen in the bis(trialkylhydrazine) **4** is calculated from the data of Ansell and Erickson¹⁶ to be 54.5° , about half way between the values found for **2** and **3**, and quite close to the tetrahedral value (as are all of the torsional angles in this compound). The strong intermolecular hydrogen bonding observed¹⁶ may well make this molecule a poor comparison with a tetraalkylhydrazine. The importance of steric effects in determining the flattening angle at nitrogen cannot, however, be overlooked.

The approximately 10° difference in the β values for **2** (θ about 180°) and **3** (θ about 70° , see below) could have significant effects on the use of photoelectron spectroscopy lone pair energy differences to estimate θ values.^{2,3} Although INDO calculations on hydrazine itself show only a 2% drop in the calculated energy difference at $\theta = 180^\circ$ when β is changed from 49 to 59° , the changes are much more significant at other θ values, about 5% at 120° , 17% at 60° , and 14% at 0° .¹⁷ The change in β as θ is changed found here ought to be incorporated into a working curve for ΔE vs. θ , as well as the experimentally found (but not predicted at the INDO level of calculation)

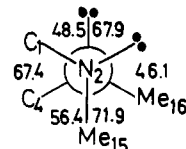


Figure 10. Newman projection along the N(2)–N(3) bond in compound 3.

insensitivity of ΔE to θ near the crossover point.¹⁸ The fact that β for other cyclic systems will be sensitive to structure seems to preclude the photoelectron spectroscopy method from being able to measure very precise θ values.

Many of the dihedral angles for **2** and **3** are shown in Figures 3 and 6. The dihedral angles about the hexahydropyridazine ring of **2** vary in roughly the manner predicted entirely from bond length considerations;^{4c} the degree of puckering is far greater at the nitrogen side of the hexahydropyridazine ring (the CN–NC angle being 9.4° larger than the 56° of cyclohexane itself) than on the opposite side (the CC–CC angle is 6.2° less than that of cyclohexane).¹⁹ We note that the internal ring torsion angle CN–NC for **2** (65.4°) is rather close to that observed for the tetrahydropyridazine **3** (67.4°). The tetrahydropyridazine is, of course, considerably flattened at the olefinic side of the six-membered ring, the torsional angle at the double bond being found to be 5.4° .

The MeN–NMe dihedral angle is about 8° larger for the axial, equatorial compound **3** (71.9°) than for equatorial, equatorial **2** (63.7°), as expected from the NMR-derived equilibrium constants,⁴ which suggested a larger Me,Me interaction in ee than in ae conformations. The MeN–NMe dihedral angle for **2**, the diequatorial compound, would have been even smaller had not β been larger for **2** than for **3**.

The lone pair–lone pair dihedral angles are of particular interest in relation to the photoelectron spectroscopy work on hydrazines.^{2,3} The lone pair electrons are not directly observed by x-ray crystallography, so only indirect estimates of the directions of the lone pair orbital axes, and hence of θ , can be made. If the lone pairs are considered to be directed perpendicular to the plane passing through the α -carbon atoms (the similarity of the C–N and N–N bond lengths makes this a reasonable procedure), $\theta = 74^\circ$ for the ae lone pairs of **3**, and 178° for the aa lone pairs of **2**. If instead, the lone pair orbital axes are considered to bisect the CNC angle in a Newman projection down the N–N bond, as illustrated in Figure 9, θ values of 69.7 and 179.2° are obtained. These two methods of estimation give approximately the same answer. The 160 – 170° θ values estimated for diequatorial hexahydropyridazines in our photoelectron spectroscopy work³ are seen to be incorrect; the lone pair–lone pair interaction does not cause torsional distortion of the hexahydropyridazine ring of the sort that would be required to obtain such a low θ value. This mistake probably arose because of our use of a constant tetrahedral β value in the ΔE vs. θ working curve, as discussed above.

Acknowledgment. We thank the National Science Foundation, both the Major Instrument Program, for funds used in purchasing the diffractometer, and for Grant MPS74-19688, for partial support of this work. W.C.H. held an Advanced Opportunity Fellowship.

Supplementary Material Available: A list of observed and calculated structure factors for **2** and **3** (14 pages). Ordering information is given on any current masthead page.

References and Notes

- (1) For an excellent review of this area through 1973, see Y. Shvo, "The Chemistry of Hydrazo, Azo, and Azoxy Groups, Part 2", S. Patai, Ed., Wiley, New York, N.Y., pp 1017–1095.

- (2) (a) P. Rademacher, *Angew. Chem.*, **85**, 410 (1973); (b) *Tetrahedron Lett.*, 87 (1974); (c) *Chem. Ber.*, **108**, 1548 (1975); (d) P. Rademacher and H. Koopman, *ibid.*, **108**, 1557 (1975).
- (3) (a) S. F. Nelsen and J. M. Buschek, *J. Am. Chem. Soc.*, **95**, 2011 (1973); (b) S. F. Nelsen, J. M. Buschek, and P. J. Hintz, *ibid.*, **95**, 2013 (1973); (c) S. F. Nelsen and J. M. Buschek, *ibid.*, **96**, 2392 (1974); (d) *ibid.*, **96**, 6982 (1974); (e) *ibid.*, **96**, 5987 (1974).
- (4) (a) S. F. Nelsen and G. R. Weisman, *J. Am. Chem. Soc.*, **96**, 7111 (1974); (b) *ibid.*, **98**, 3281 (1976); (c) G. R. Weisman and S. F. Nelsen, *ibid.*, **98**, 7007 (1976).
- (5) S. F. Nelsen and E. L. Clennan, manuscript in preparation.
- (6) H. Christol, D. Fevrier-Piffaretti, and Y. Pietrasanta, *Bull. Soc. Chim. Fr.*, 2439 (1972).
- (7) R. A. Sparks, "Operations Manual, Syntex P1 Diffractometer", Syntex Analytical Instruments, Cupertino, Calif., 1970.
- (8) T. H. Whitesides, R. V. Slaven, and J. Calabrese, *Inorg. Chem.*, **13**, 1895 (1974).
- (9) Programs used in the structural determination: MULTAN (G. Germain, P. Main, and M. M. Woolfson, *Acta Crystallogr., Sect. B*, **26**, 274 (1974)); data reduction and merging, Fourier calculations and least squares (J. Calabrese); ORTEP2 (C. K. Johnson, *U.S.A.E.C., ORNL-3794*, 1 (1970)).
- (10) $R_1 = \frac{[\sum |F_o| - |F_c|] / \sum |F_o|}{[\sum w_i / |F_o|^2 - |F_c|^2]^{1/2}} \times 100\%$ and $R_2 = \frac{[\sum w_i / |F_o| - |F_c|]^2}{[\sum w_i / |F_o|^2]^{1/2}} \times 100\%$.
- (11) All least-squares refinements³ were based on the minimization of $\sum w_i (|F_o| - |F_c|)^2$ with the weights w_i set equal to $1/\sigma(F_o)^2$. The estimated standard deviations given in the tables and figures in this paper were calculated from the full variance-covariance matrix of the final refinement cycle.
- (12) R. Allman, "The Chemistry of Hydrazo, Azo, and Azoxy Groups, Part 1", S. Patai, Ed., Wiley, New York, N.Y., p 20.
- (13) R. L. Collins and W. N. Lipscomb, *Acta Crystallogr.*, **4**, 10 (1951).
- (14) A. Yamaguchi, I. Idishima, T. Shimaniuchi, and S.-I. Mizushima, *J. Chem. Phys.*, **31**, 843 (1959).
- (15) Y. Marino, I. Iijima, and Y. Murata, *Bull. Chem. Soc. Jpn.*, **33**, 46 (1960).
- (16) G. B. Ansell and J. L. Erickson, *J. Chem. Soc., Perkin Trans. 2*, 270 (1975). We note that the sign of the z coordinate of H(5) is given wrong in Table I of this paper.
- (17) Interpolated from calculations reported in Table II, ref 3d.
- (18) S. F. Nelsen, V. Peacock, and G. R. Weisman, *J. Am. Chem. Soc.*, **98**, 5269 (1976).
- (19) For reviews of internal torsional angles in six-membered heterocycles, see (a) J. B. Lambert, *Acc. Chem. Res.*, **4**, 87 (1971); (b) R. Bucourt, *Top. Stereochem.*, **9**, 159 (1974).

Carbon-13 Nuclear Magnetic Resonance Studies of Vitamin B₆ Schiff Base and Carbinolamine Formation in Aqueous Solution.¹ 1. The Adduct of Pyridoxal 5'-Phosphate and DL-Alanine

Byeong H. Jo, Vasu Nair, and Leodis Davis*²

Contribution from the Department of Chemistry, University of Iowa, Iowa City, Iowa 52242. Received August 5, 1976

Abstract: The Schiff base and carbinolamine formation from pyridoxal 5'-phosphate and DL-alanine in aqueous solution was investigated by carbon-13 nuclear magnetic resonance spectroscopy. The pK_a value for the deprotonation of the pyridinium nitrogen was found to be less than that of free pyridoxal 5'-phosphate. At pH 7.1 two pH-dependent forms of the Schiff base and three species of carbinolamines which have different configurations were detected, while at pH 10.5 the pH-dependent forms of the Schiff base predominate. At pH 6.3 the Schiff base is equally distributed between the pH-dependent forms and increased concentration of the three carbinolamine species were detected. Evidence presented suggests that the Schiff bases allow for no intramolecular interactions between the iminium proton and either the phenolate anion of C-3 of pyridoxal 5'-phosphate or the carboxyl group of the amino acid. At pH 12.8, the equilibrium is shifted from the Schiff base toward free components and the carbinolamine intermediate was not clearly detected.

Vitamin B₆ compounds are known to be essential in enzymatic metabolism of amino acids. The early studies by Braunstein et al.³ and Snell et al.⁴ suggested that the initial step in the metabolic mechanism of amino acids is Schiff base formation between the formyl group of pyridoxal 5'-phosphate and the amino group of the amino acid.

Considerable information on the equilibrium of Schiff bases formed by pyridoxal or pyridoxal 5'-phosphate with amino acids or amines has been obtained from UV-visible and ¹H NMR studies in aqueous and nonaqueous media,⁵⁻¹⁴ but structural evidence for these dynamic states has not been conclusive. Furthermore, the tetrahedral intermediate (carbinolamine) formed through the addition process between the carbonyl and the amino group of the two components has received little structural attention.

Recent studies of vitamin B₆ and derivatives^{15,16} and amino acids^{17,18} by carbon-13 nuclear magnetic resonance spectroscopy (¹³C NMR) have led us to pursue the application of ¹³C NMR methods for the derivation of dynamic structural information in the formation of Schiff bases and carbinolamine complexes from pyridoxal 5'-phosphate and amino acids.

This study is the first comprehensive treatment of ¹³C NMR application to Schiff base and carbinolamine formation from pyridoxal 5'-phosphate and amino acids, although a preliminary study on pyridoxal 5'-phosphate-amine systems was re-

ported very recently.^{19,20} We wish to establish a correlation of chemical shifts with Schiff base structures and to provide ¹³C NMR evidence for the intermediacy of carbinolamines.

Experimental Section

Pyridoxal 5'-phosphate was purchased from Sigma Chemical Co. and DL-alanine was obtained from Merck and Co. Reagents were used without further purification. D₂O obtained from Diaprep was 99.7% pure. The NaOD was prepared from D₂O and metallic sodium under dry nitrogen.

¹³C NMR spectra were obtained at 25 °C on a Bruker HX90E pulse Fourier transform NMR spectrometer (22.63 MHz) interfaced with a Nicolet 1080 computer. Typical parameters for ¹³C NMR experiments follow: spectral width of 6024 Hz with acquisition of 8 K data points, 7-μs pulse corresponding to a tip angle of 30°, and a recovery time of 2 s. The number of spectral accumulations was in the range of 5000-7500 depending on sample conditions. Chemical shifts are given in parts per million (ppm) downfield from external tetramethylsilane (capillary with 5-mm o.d. concentric tube within the 10-mm sample tube). The digital reproducibility is ±0.1 ppm. The probe temperature was 25 °C. D₂O solvent was the source of an internal deuterium lock. Broad band proton noise decoupling and gated decoupling experiments were carried out by standard methods.

The sample solution was prepared by first dissolving the amino acid in the 0.35 M pyridoxal 5'-phosphate (pH 6.0) stock solution and then adjusting to the final concentration and pH. Sample concentrations were 0.3 M in each component. Before preparing the stock solution,